Applied Catalysis B: Environmental 158–159 (2014) 296–300

Contents lists available at ScienceDirect

Applied Catalysis B: Environmental

journal homepage: www.elsevier.com/locate/apcatb

Surface-phase junctions of branched TiO_2 nanorod arrays for efficient photoelectrochemical water splitting

Jiao Liu[a,b], Xuelian Yu[a], Qingya Liu[b], Rongji Liu[a,c], Xinke Shang[a,c], Shuangshuang Zhang[a,c], Wenhui Li[a,d], Wanquan Zheng[d], Guangjin Zhang[a,*], Hongbin Cao[a,*], Zhanjun Gu[e]

[a] Key Laboratory of Green Process and Engineering, Institute of Process Engineering, Chinese Academy of Sciences, 100190 Beijing, China
[b] Beijing University of Chemical Engineering, 100029 Beijing, China
[c] University of Chinese Academy of Sciences, 100049 Beijing, China
[d] Institute for Interdisciplinary Research, Jianghan University, 430056, Wuhan, China
[e] Key Laboratory for Biomedical Effects of Nanomaterials and Nanosafety, Institute of High Energy Physics, Chinese Academy of Sciences, 100049 Beijing, China

ARTICLE INFO

Article history:
Received 25 February 2014
Received in revised form 18 April 2014
Accepted 20 April 2014
Available online 30 April 2014

Keywords:
Surface-phase junction
Branched TiO_2 nanorod array
Photoanode
Water splitting
Charge transfer

ABSTRACT

Flower-like branched TiO_2 nanorod arrays (NRs) owning the surface anatase/rutile junctions on FTO substrates with operational diameter were successfully fabricated by a modified hydrothermal method. Transmission electron microscopy, Raman spectroscopy, field emission scanning electron microscopy, and X-ray diffraction revealed a unique flower-like ranched morphology, surface features, a crystal phase, and lattice constant of TiO_2. Photoelectrochemical (PEC) measurements showed excellent photocatalytic properties of the flower-like branched TiO_2 NRs. The surface phase formed between anatase and rutile TiO_2 NRs which efficiently enhances the separation of photo-generated electron–hole pairs and accelerates the transport of charges is the key influence factor. The results suggest that the branched TiO_2 NRs owning the surface anatase/rutile junctions are very promising platform to make highly efficient photoanodes for energy devices.

1. Introduction

Semiconductor photocatalysts have attracted much research attention because of their applications to solar energy conversion and environmental purification in the past decades [1–3]. Among photocatalysts, TiO_2 as one of the most important transition metal oxides owning a favorable band edge position, nontoxicity, a strong optical absorption, and an inexpensive cost [4–8]. The photocatalytic performance of TiO_2 has been influenced by many factors such as the phase structure, the surface area, the crystallite size, and the amount of surface hydroxyl groups, and so on [9–12]. Among them, the restriction of recombination between electrons and holes is one of the key issues so as to enhance photocatalytic efficiency [13,14]. So it is highly desirable to develop approaches that can validly promote charge separation in TiO_2 [15,16]. Various methods, such as synthesizing branched structures [17], doping with metal or non-metal elements [18,19], post-growth hydrogen annealing [20], sensitizing with other small band gap semiconductor materials [21], and controlling its crystallite size and structure [22,23], have been studied to improve the photocatalytic properties of TiO_2 nano-materials. It is well-known that anatase and rutile TiO_2 as the two major crystalline phases are mostly used in photocatalytic reactions [24], and the most significant factor that influences the photocatalytic performance of TiO_2 is its crystal form [15,16]. Anatase is generally accepted to be more efficient than rutile and the mixtures of the TiO_2 polymorphic phases (such as commercial Degussa P25) often show photocatalytic activities superior to those of the pure phases. The mixtures of the TiO_2 polymorphic phases are usually beneficial to enhance the photocatalytic activity due to the different energy levels for their corresponding conduction and valence bands [25]. Fabrication surface-phase junctions of TiO_2 particles, has been demonstrated to be a valid strategy in photocatalytic performance. The report by Can Li et al. shows that the photocatalytic activity of TiO_2 was enhanced up significantly due to the surface-phase junctions which is of great benefit to obtain efficient charge separation [26].

Besides, for photoelectrochemical water splitting, the main challenge is the design of photoanode materials with improved solar-to-hydrogen conversion efficiency. The traditional

* Corresponding authors. Tel.: +86 10 62528935; fax: +86 10 62528935.
E-mail addresses: zhanggj@home.ipe.ac.cn (G. Zhang), hbcao@home.ipe.ac.cn (H. Cao).

http://dx.doi.org/10.1016/j.apcatb.2014.04.032
0926-3373/

photoanode that is made by TiO_2 nanoparticles suffers from high charge recombination loss. Due to huge electron trapping/scattering at grain boundaries, the electron mobility in a nanoparticle film is only 1% of that of bulk single crystal. Thus, one-dimension (1D) nanostructure such as nanorods and nanotubes (NTs) have received more attention because of their advantage in charge transport [27]. However, most of the prepared 1D nanostructure have only one crystal phase (rutile or anatase). Thus, it is highly desirable to synthesize a 1D nanostructure owning the two phases, which can certainly enhance the charge separation and transportation. To date, it is still a real challenge to make such branched TiO_2 NRs which own the surface-phase junctions aimed at effective photoelectrochemical water splitting.

In this study, branched TiO_2 NRs which own the surface anatase/rutile junctions were successfully synthesized via a simple modified hydrothermal method. PEC measurement shows that the photoelectrical response was increased significantly with the surface phase junction and the highest photocurrent density of 1.02 mA/cm^2 is observed at 0.8 V vs. RHE when the photoelectrode is illuminated by solar simulator (AM 1.5G). The enhanced charge separation and transportation on surface-phase junctions of TiO_2 NRs contribute to the high efficient photoelectrochemical water splitting. Thus, the branched TiO_2 NRs owning surface-phase junctions could emerge as viable alternatives to traditional single-crystalline TiO_2 NRs for photoanode materials.

2. Experimental

2.1. Growth of TiO_2 NRs and branched TiO_2 NRs

The TiO_2 nanorods were synthesized by a hydrothermal method. The FTO substrate (2.5 cm × 5 cm) ultrasonically cleaned in ethanol and acetone in turn for 3 times was immersed into $TiCl_4$ aqueous solution for half an hour to form a seed layer [28]. In a typical synthesis, 15 ml deionized water was mixed with 2.5 ml NaCl saturated aqueous solution and 15 ml HCl aqueous solution (36–38%) under magnetic stirring for 10 min. The seeded-FTO substrate was put in the above solution sideling poured into a Teflon-lined stainless steel autoclave (50 mL capacity). The hydrothermal synthesis was conducted at 120–150 °C for 15–18 h [23], the autoclave was cooled to room temperature naturally. The obtained samples were washed with deionized water and dried at 80 °C in air. For branched TiO_2 NRs, the prepared TiO_2 nanorods was further put into an aqueous solution mixed by Ammonium hexafluo-rotitanate ($[NH_4]_2TiF_6$) and boric acid (H_3BO_3) for certain times at room temperature [29].

2.2. Characterizations

The products were characterized with a D/max 2500, Rigaku, and X-ray diffraction (XRD) instrument with high-intensity Cu Kα1 irradiation (l = 1.5406 Å). The Raman spectra were measured using laser confocal micro-Raman spectroscopy (Renishaw Raman system). For scanning electron microscopy (SEM) test, the TiO_2 NRs or branched TiO_2 NRs synthesized on the FTO substrate were directly used, and the SEM analysis was performed on a Hitachi model S-4300 field-emission scanning electron microscope (FESEM). For preparing the transmission electron microscope (TEM) samples, the TiO_2 NRs or branched TiO_2 NRs were scraped off from the FTO substrate and further dispersed in ethanol, and the TEM analysis was obtained using a JEOL JEM-2100F at an acceleration voltage of 200 kV. The UV–vis absorption spectra were recorded with a Hitachi 3010 spectrophotometer.

2.3. Photoelectrochemical measurements

The PEC properties were investigated using a Keithley 2611 digital source meter. The light source was a 150 W xenon lamp (Sciencetech, SS150) calibrated to 100 mW/cm^2 with a standard Si solar cell. CHI760D CH electrochemical station was used for linear sweep voltammetry (I–V) and amperometry (I–t) measurements. Incident photon to current conversion efficiencies (IPCEs) were calculated from amperometry measurements using a monochromator (Newport) in conjunction with a power meter and photodiode (Newport). The as-prepared sample, the platinum (Pt) sheet, and the reversible hydrogen electrode (RHE) were used as working electrode, counter electrode, and reference electrode, respectively. An aqueous solution containing 1.0 M KOH was used as an electrolyte. The illuminated area of the working electrode is 0.3 cm × 0.3 cm.

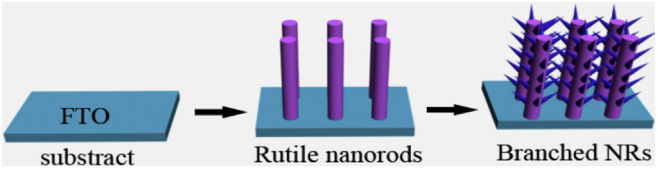

Scheme 1. The procedure for the synthesis step of branched TiO_2 NRs.

3. Results and discussion

3.1. Morphology and structure of TiO_2 NRs and branched TiO_2 NRs

Branched TiO_2 NRs on the FTO substrate were synthesized via a two-step growth process, as shown in Scheme 1. By a hydrothermal method which has been well developed in the past, the TiO_2 NRs on FTO substrates were prepared. The morphologies of the TiO_2 NRs are shown in Fig. 1a, showing the average diameter of nanorods is 70 nm and the surface of nanorods is very smooth with coverage density around 6 × 10^9 NRs/cm^2. The inset SEM image of Fig. 1a is a cross-sectional view of the same sample showing that the nanorods are nearly vertical to the FTO substrate and about 2 μm in length. Lattice fringes with interplanar spacing 0.324 nm, 0.291 nm and 0.230 nm can be index to the (1 1 0), (0 0 1) and (1 0 0) faces of tetragonal rutile phase. The results indicate that the prepared NRs are single-crystalline tetragonal rutile-phase TiO_2 with a [0 0 1] and [1 0 0] growth direction.

Flower-like branched TiO_2 NRs were successfully formed by treating prepared NRs in aqueous solutions mixed by 0.015 M ammonium hexafluo-rotitanate ($[NH_4]_2TiF_6$) and 0.075 M boricacid (H_3BO_3) under room temperature for different time: 40 h, 80 h, 120 h. The morphologies of the branched TiO_2 NRs obtained by 40 h's treatment are shown in Fig. 1c. It can be observed that short needle-shaped branches were grown uniformly on the entire surface of NRs trunks. The inset of Fig. 1c is a cross-sectional view of the same sample showing that the branched NRs are still vertical to the FTO substrate and the branches can be observed. The specific surface area and roughness factor of the TiO_2 NRs were significantly improved, which benefits to their catalytic performance. With the increase of growth time to 120 h, the densities of the branches increased to reach full coverage of the whole surface (Fig. S1). The crystal structure of branched NRs was further characterized by TEM and high resolution TEM (HRTEM). Fig. 1d–g are SEM, TEM and HRTEM images of branched TiO_2 NRs by treating in the mixed aqueous solutions for 40 h. It can be observed that branches densely and uniformly covered the surface of NRs. Close observation of the branches (Fig. 1d) indicates that the branches possess a cone shape with an average length of 40 nm, a base diameter around 34 nm. HRTEM of the single branch shows well resolved lattice fringes, suggesting good crystallinity of the branches. The lattice fringes with interplanar spacing 0.352 nm indicate the branches are single-crystalline tetragonal anatase-phase TiO_2. And the branches grow along with [1 0 0] directions. The HRTEM of the trunk of branched

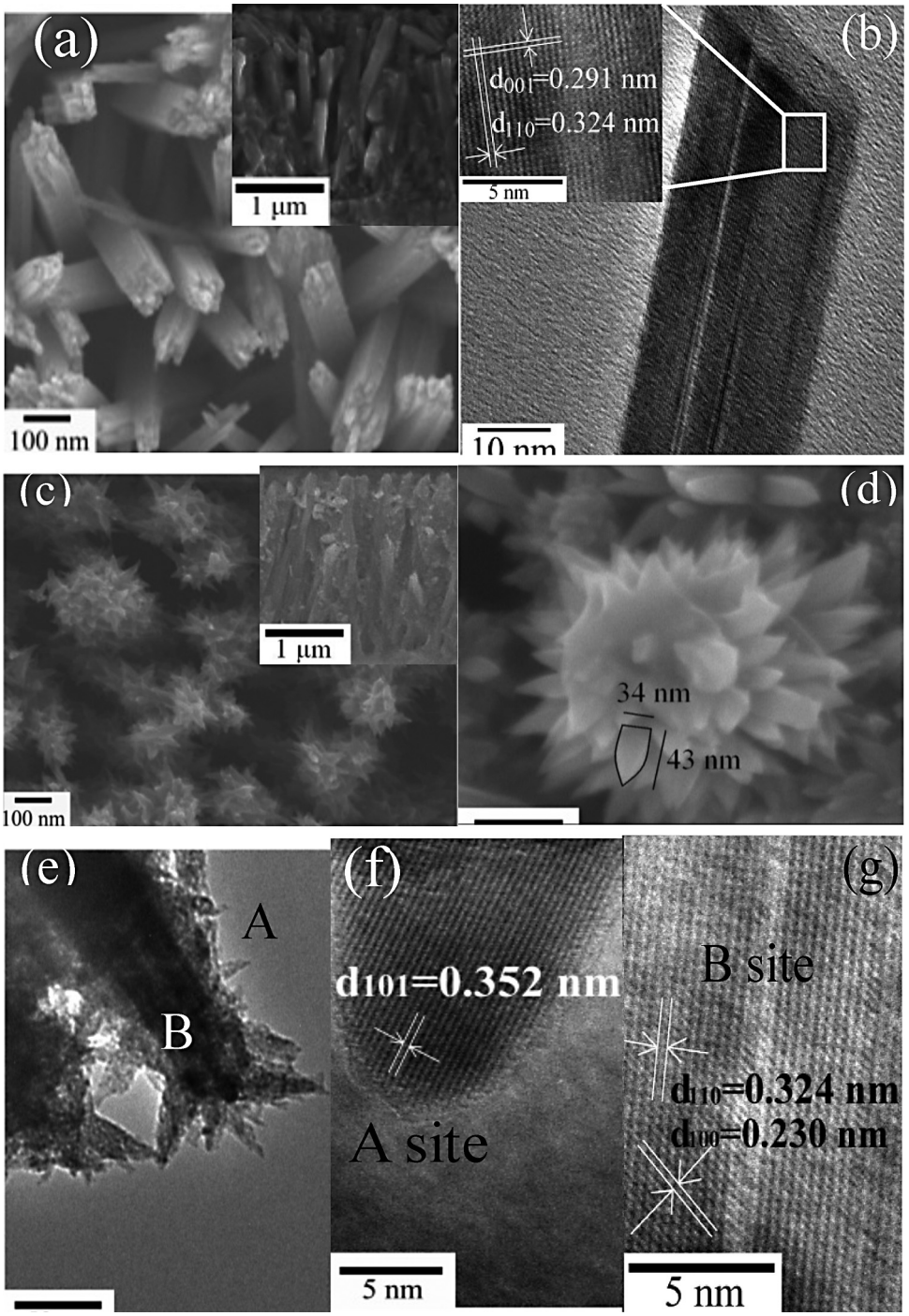

Fig. 1. Typical top view SEM and HRTEM images of TiO_2 NRs and branched TiO_2 NRs: (a) TEM and (b) HRTEM image of bare NRs, (c) TEM and (d) SEM image of branched NRs, (e) TEM, (f) HRTEM and (g) HRTEM image of a single branched nanorod. The inset of (a) and (c) shows SEM images of a cross-sectional view of the well aligned TiO_2 NRs and branched TiO_2 NRs.

NRs confirmed it was rutile-phase TiO_2 with [001] growth direction. Thus the surface anatase/rutile junctions were formed at the boundary of branches and trunks. The HRTEM visualized the surface-phase junction and give the direct evidence for the surface anatase/rutile junctions formed on branched TiO_2 NRs. To the best of our knowledge, this is the first example of branched NRs with surface anatase/rutile junctions.

In order to further identify the phase junctions of the branched TiO_2 NRs, the prepared samples on FTO substrates were further characterized by XRD and Raman spectrum. As shown in Fig. 2a, the observed characteristic peaks at 26.6°, 36.1°, 38.8°, 63.0° are assigned to the (110), (101), (200) and (002) planes of rutile phase of TiO_2 (JCPDS No. 21-1276). This observation is also consistent with the HRTEM shown in Fig. 1b. For the branched TiO_2 NRs, in addition to those diffraction peaks that assigned to rutile phase of TiO_2, new peaks at 48.1° and 53.9° that can be index to (200) and (105) planes of anatase of TiO_2 were appeared (JCPDS No. 89-4921). The relative low amount of branches compared with the trunk make it hard to be observed with other diffraction peaks of anatase phase of TiO_2 crystals. Compared with the other diffraction peaks, the (200) diffraction peak is significantly enhanced. Again, the strong diffraction peaks of (200) plane indicate the branches

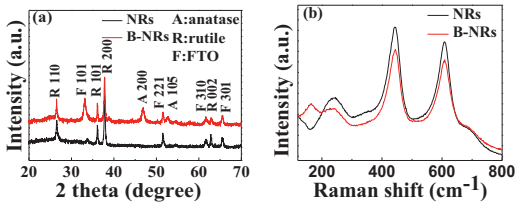

Fig. 2. XRD patterns (a) and Raman spectra (b) for the bare TiO_2 and the branched TiO_2 NRs (disposed 40 h).

grow along with [1 0 0] direction, which is also consistent with HRTEM observations that are shown in Fig. 1f.

Further characterization studies provide convincing evidence for the phase of anatase of the TiO_2 nano-branched arrays. Raman spectra of the TiO_2 nano-branched arrays are shown in Fig. 2b. The bare TiO_2 arrays showed Raman peaks at 245 cm^{-1}, 442 cm^{-1}, and 609 cm^{-1}, which is a typical feature of rutile phase. For the branched TiO_2 NRs, a Raman peak of anatase phase at 161 cm^{-1} was observed. These results confirmed the formation of new anatase-phase branches on those rutile-phase TiO_2 NRs. Besides, with the increase of growth time of TiO_2 NRs, the stronger peak at 161 cm^{-1} was observed, indicating that more phase of anatase was obtained (see Fig. S2 for detail).

3.2. Photoelectrochemical water splitting performance

PEC performance of the bare TiO_2 NRs and branched NRs supported on FTO were studied to demonstrate the higher photocatalytic activity of the branched NRs photoanodes with surface phase junctions. One key measurement used was that of current density versus potential (J–V) curves under simulated solar illumination (AM 1.5G, 100 mW/cm^2). The J–V curves of the TiO_2 films supported on FTO were measured in 1 M KOH using a standard three-electrode configuration. The photoelectrochemical responses of the bare TiO_2 NRs and branched TiO_2 NRs film are shown in Fig. 3a. When sweeping the potential anodically, the branched NRs showed a sharp increase of the current and reached prompt saturation of the photocurrent density at 0.2 V vs. RHE. Under illumination from the solar simulator, the bare TiO_2 NRs showed small photocurrent density, in which the maximum value was 0.43 mA/cm^2 at 0.8 V vs. RHE. However, the branched TiO_2 NRs photoanodes show greatly enhanced photocurrent values, and the large saturated photocurrent density of 1.02 mA/cm^2 is observed at 0.8 V vs. RHE. This represents more than a 2-fold increase in the current density over the measurement performed in the bare TiO_2 NRs, suggesting much more efficient charge separation and collection than in the bare TiO_2 NRs. The better performance of branched NRs is also revealed by its more negative onset potential. Compared with bare NRs, the onset potential of branched NRs shifted from 0.13 V to 0 V vs. RHE. The onset potentials of the TiO_2 photoelectrodes can be taken as a measure of quasi-Fermi levels of the anodic

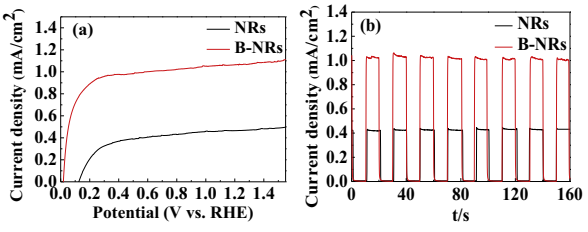

Fig. 3. (a) Current density versus potential curves of the bare TiO_2 and the branched TiO_2 NRs after branch growth with 40 h, (b) time-dependent photocurrent density of bare/branched TiO_2 NRs (disposed 40 h) at repeated on/off cycles of simulated sunlight illumination.

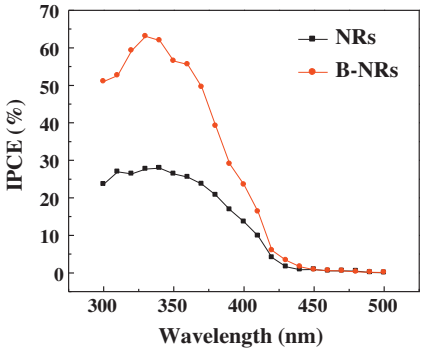

Fig. 4. IPCE plots of bare/branched TiO_2 NRs (deposit for 40 h) measured at an applied bias of 0.3 V.

photocurrent. The migration of excited electrons from the anatase conduction band to that of rutile is energetically possible given the lower conduction band level of the latter. The big negative shift of the onset potential requires intimate physical interaction between the two phases. The existence of the surface anatase/rutile junctions certainly contributes to such onset potential shift. Besides, as described above, when the growth time increased to 120 h, the whole surface of rutile nanorods was covered homogeneously by anatase layer (Fig. S1d). The photoelectrochemical responses of this sample was also examined and compared with that of branched TiO_2 NRs film (Fig. S3). This sample showed much worse photoelectrochemical response than branched NRs. This further conformed that the branched TiO_2 NRs owning the surface anatase/rutile junctions showed excellent photocatalytic properties.

Furthermore, the chemical and structural stability during PEC water splitting is another important factor to evaluate concerning the potential PEC materials. Time-dependent measurement carried out on a representative branched TiO_2 NRs displayed a highly stable photocurrent density of ~1.02 mA/cm^2 at an applied bias of 0.8 V vs. RHE with 8 repeated on/off cycles correlated to the simulated solar light as shown in Fig. 3b, in which the photocurrent was observed to be almost consistent and repeatable. By contrast, the pure rutile TiO_2 NRs displayed a lower stable photocurrent density of ~0.43 mA/cm^2 under the same conditions. Rectangular shaped photocurrent transients indicate a strongly decreased electron back recombination and a good reproducibility of the photoanodic processes.

Incident photon to current conversion efficiencies (IPCEs) of the two samples were measured at 0.3 V vs. RHE from amperometry measurements using a monochromator in conjunction with a power meter and photodiode, given by:

$$\mathrm{IPCE} = \frac{1240 J_{ph}}{\lambda I} \times 100\%$$

where J_{ph} is the steady-state photocurrent density (mA/cm^2) at a specific wavelength, λ is the wavelength (nm) of the incident light, I is the light power intensity (mW/cm^2) of the wavelength at the film surface. The maximum IPCE for the branched TiO_2 NRs can reach 62% at 340 nm, higher than that of the bare TiO_2 NRs which have a maximum IPCE of 26% at 340 nm as shown in Fig. 4.

3.3. Light absorption and proposed photocatalytic mechanism

To account for such high performance, light absorption properties of the branched NRs as well as the pure NRs were studied. As shown in Fig. 5a, the absorption range of the branched TiO_2 NRs is below 400 nm and is very close to that of the bare TiO_2 NRs. As the light absorption determines the charge generation efficiency, the results indicate the two photoanode have close charge

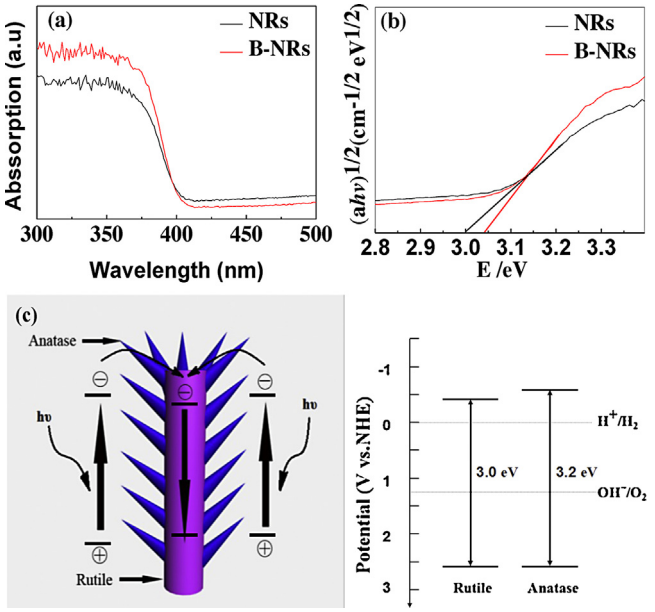

Fig. 5. (a) Diffuse reflection spectra and (b) plots of the transformed Kubelka–Munk function versus the energy of light over the bare TiO_2 and the branched TiO_2 NRs after branch growth with 40 h, (c) schematic drawing of the photocatalytic mechanism of the branched TiO_2 NRs with enhanced charge-separation efficiency and (d) electrochemical potentials (vs. NHE) of the band edges of anatase and rutile.

generation efficiency. Another key factor that affects the PEC activity is charge separation and transport efficiency. The fact that the conduction band edge of branched TiO_2 NRs is higher than that of the bare TiO_2 NRs is thought to facilitate interfacial electron transfer, as shown in Fig. 5b, due to the formation of anatase phase on the rutile trunk. The precise band diagram of anatase-rutile junction has shown in Fig. 5d. The charge transfer from anatase to rutile due to the slightly lower conduction band energy of rutile [30], should be responsible for the improvement of the photocatalytic activity. Photogenerated electron hole pairs in the anatase branches can be separated by transferring the electron to the rutile-phase trunk and the energy barrier would suppress back electron transfer. Consequently, the holes left in the valence band of anatase phase in the surface of branched TiO_2 NRs (Fig. 5c), efficiently increased the lifetimes of carriers and enhanced PEC performance [31,32]. In addition, the rough surface of the branched NRs facilitates the hole transfer at TiO_2/electrolyte interface and thus increases the charge collection efficiency. All these factors make the branched NRs exhibit excellent PEC performance.

All the above results indicate that the branched TiO_2 NRs owning surface anatase/rutile junctions exhibit much better photoelectrochemcial water splitting activity than the NRs owning pure phase. In addition, compared with literature, the saturation photocurrent achieved is also much better than those reported pure TiO_2 nanostructure photoanodes [33] and even the nanotube array films with the thickness of 6 μm (see Table S1 for detail) [34], This illustrates the advantage of the branched NRs owning surface anatase/rutile junctions over other nanostructured platforms for PEC water splitting applications.

In addition, the current branched NRs also showed better performance with sensitization by quantum dots. As shown in Fig. S4, after the sensitization with CdS–ZnS QDs by the reported methods [35], the saturation photocurrent increased to 2.3 mA/cm^2 at 1 V vs. RHE. In comparison, for the bare NRs, the saturation photocurrent just increased to 0.7 mA/cm^2 at 1.5 V vs. RHE. It should be noted that our sensitization have not been fully optimized and hopefully it can be further improved to get better PEC performance.

4. Conclusions

In summary, for the first time, flower-like branched TiO_2 nanorod arrays owning the surface anatase/rutile junctions were successfully synthesized. The branched NRs showed much better PEC performance than the bare NRs and other reported pure phase of TiO_2 nanostructures. The surface anatase/rutile junctions formed on the boundary of branches and trunks serve as charge separating site and thus improved the PEC performance. Further sensitization of branched NRs by quantum dots can significantly improve its PEC activity. This work provides a promising platform as viable alternatives to traditional single-crystalline TiO_2 NRs for highly efficient photocatalysts or anodes of energy devices.

Acknowledgements

This work was supported by the National Natural Science Foundation of China (No. 21371173), National Basic Research Programs of China (973 program, No. 2012CB932504).

Appendix A. Supplementary data

Supplementary data associated with this article can be found, in the online version, at http://dx.doi.org/10.1016/j.apcatb.2014.04.032.

References

[1] R. Wang, K. Hashimoto, A. Fujishima, M. Chikuni, E. Kojima, A. Kitamura, M. Shimohigoshi, T. Watanabe, Nature 388 (1997) 431–432.
[2] M. Grätzel, Nature 414 (2001) 338–344.
[3] P.V. Kamat, Chem. Rev. 93 (1993) 267–300.
[4] A. Fujishima, K. Honda, Nature 238 (1972) 37–38.
[5] B. O'regan, M. Grfitzeli, Nature 353 (1991) 737–740.
[6] M. Liu, X. Qiu, M. Miyauchi, K. Hashimoto, Chem. Mater. 23 (2011) 5282–5286.
[7] A.L. Linsebigler, G. Lu, J.T. Yates Jr., Chem. Rev. 95 (1995) 735–758.
[8] N.-L. Wu, S.-Y. Wang, I. Rusakova, Science 285 (1999) 1375–1377.
[9] P. Mishra, O. Srivastava, Bull. Mater. Sci. 31 (2008) 545–550.
[10] P. Roy, S. Berger, P. Schmuki, Angew. Chem. Int. Ed. 50 (2011) 2904–2939.
[11] C. Bernardini, G. Cappelletti, M.V. Dozzi, E. Selli, J. Photochem. Photobiol. A: Chem. 211 (2010) 185–192.
[12] V. Puddu, H. Choi, D.D. Dionysiou, G.L. Puma, Appl. Catal. B: Environ. 94 (2010) 211–218.
[13] A. Rivera, K. Tanaka, T. Hisanaga, Appl. Catal. B: Environ. 3 (1993) 37–44.
[14] Z. Ding, G. Lu, P. Greenfield, J. Phys. Chem. B 104 (2000) 4815–4820.
[15] K.E. Karakitsou, X.E. Verykios, J. Phys. Chem. 97 (1993) 1184–1189.
[16] H. Tada, M. Tanaka, Langmuir 13 (1997) 360–364.
[17] I.S. Cho, Z. Chen, A.J. Forman, D.R. Kim, P.M. Rao, T.F. Jaramillo, X. Zheng, Nano Lett. 11 (2011) 4978–4984.
[18] S. Hoang, S. Guo, N.T. Hahn, A.J. Bard, C.B. Mullins, Nano Lett. 12 (2011) 26–32.
[19] C. Das, P. Roy, M. Yang, H. Jha, P. Schmuki, Nanoscale 3 (2011) 3094–3096.
[20] G. Wang, H. Wang, Y. Ling, Y. Tang, X. Yang, R.C. Fitzmorris, C. Wang, J.Z. Zhang, Y. Li, Nano Lett. 11 (2011) 3026–3033.
[21] X. Yu, R. Liu, G. Zhang, RSC Adv. 3 (2013) 8351–8355.
[22] K. Shankar, J.I. Basham, N.K. Allam, O.K. Varghese, G.K. Mor, X. Feng, M. Paulose, J.A. Seabold, K.-S. Choi, C.A. Grimes, J. Phys. Chem. C 113 (2009) 6327–6359.
[23] B. Liu, E.S. Aydil, J. Am. Chem. Soc. 131 (2009) 3985–3990.
[24] J. Zhu, W. Zheng, B. He, J. Zhang, M. Anpo, J. Mol. Catal. A: Chem. 216 (2004) 35–43.
[25] A. Di Paola, G. Cufalo, M. Addamo, M. Bellardita, R. Campostrini, M. Ischia, R. Ceccato, L. Palmisano, Colloids Surf. A: Physicochem. Eng. Aspects 317 (2008) 366–376.
[26] J. Zhang, Q. Xu, Z. Feng, M. Li, C. Li, Angew. Chem. Int. Ed. 47 (2008) 1766–1769.
[27] H.J. Yun, H. Lee, J.B. Joo, W. Kim, J. Yi, J. Phys. Chem. C 113 (2009) 3050–3055.
[28] J. Wang, T. Zhang, D. Wang, R. Pan, Q. Wang, H. Xia, J. Alloys Compd. 551 (2013) 82–87.
[29] Y. Masuda, T. Ohji, K. Kato, Cryst. Growth Des. 10 (2009) 913–922.
[30] H. Tang, K. Prasad, R. Sanjines, P. Schmid, F. Levy, J. Appl. Phys. 75 (1994) 2042–2047.
[31] T. Kawahara, Y. Konishi, H. Tada, N. Tohge, J. Nishii, S. Ito, Angew. Chem. 114 (2002) 2935–2937.
[32] J. Tian, R. Gao, Q. Zhang, S. Zhang, Y. Li, J. Lan, X. Qu, G. Cao, J. Phys. Chem. C 116 (2012) 18655–18662.
[33] X. Feng, K. Shankar, O.K. Varghese, M. Paulose, T.J. Latempa, C.A. Grimes, Nano Lett. 8 (2008) 3781–3786.
[34] Z. Zhang, M.F. Hossain, T. Takahashi, Int. J. Hydrogen Energy 35 (2010) 8528–8535.
[35] U. Shaislamov, B.L. Yang, Int. J. Hydrogen Energy 38 (2013) 14180–14188.